Partial Structures of Fully Dehydrated $Ni_{30}Na_7Cl_{12}Si_{137}Al_{55}O_{384}$ (Solid-State Nickel(II)-Exchanged Zeolite Y) and of Its D_2O Sorption Complex by Pulsed-Neutron Diffraction

Razeen M. Haniffa and Karl Seff*

Department of Chemistry, University of Hawaii, 2545 The Mall, Honolulu, Hawaii 96822

Received: September 25, 1997; In Final Form: December 16, 1997

Ni^{2+}-exchanged zeolite Y was prepared by solid-state ion-exchange methods ($Ni_{30}Na_7Cl_{12}Si_{137}Al_{55}O_{384}\cdot nH_2O$ per unit cell) and was fully dehydrated (Ni_{30}−Y). Rehydration with D_2O and evacuation at 24 °C yielded a second sample (Ni_{30}−Y·D_2O). Pulsed-neutron diffraction data were collected at 15 K; the structures were determined in the space group *Fd*3*m*; R_p = 0.0212 and 0.0184 and R_{wp} = 0.0287 and 0.0257 for the two structures, respectively. In Ni_{30}−Y, 30 Ni^{2+} ions occupy 4 crystallographic sites: four ions are found at site I, at the centers of double 6-rings; 18 occupy two I′ sites, outside double 6-rings, 2.09(1) and 2.50(2) Å, respectively, from three nearest-framework oxygens; 8 are located at site II′, adjacent to a single 6-ring, 2.13(1) Å from three nearest-framework oxygens. Sites I′ and II′ are both 3-fold-axis sodalite-unit positions. The 12 Cl^- ions each bridge between two site-I′ Ni^{2+} ions (Ni−Cl = 2.60(1) and 2.73(4) Å); each Cl^- ion is 2.93(2) Å from two framework oxygens and 3.14(2) Å from two other framework oxygens. Six of the eight sodalite units per unit cell contain a $(NiClNiClNi)^{4+}$ cluster. The two remaining sodalite units each contain four Ni^{2+} ions tetrahedrally arranged at site II′. In Ni_{30}−Y·D_2O, the 30 Ni^{2+} ions are located as follows: 4 at site I, 11 at site I′, 4 at site II′, and 11 at site III′ in the supercage. Five of the sodalite units contain one Ni(I′) ion, each coordinated octahedrally to three D_2O molecules and to three framework oxygens; three sodalite units contain two octahedral Ni(I′) ions, each coordinated to one terminal D_2O molecule, two bridging D_2O molecules, and three framework oxygens. Each site-III′ Ni^{2+} ion coordinates to four framework oxygens in a distorted square-planar manner. A deuterium atom of a water molecule coordinated to each site-III′ Ni^{2+} ion hydrogen bonds to a framework oxygen (D−O = 1.75(4) Å). It is clear that the exchange of NH_4^+ for Na^+ in the initial step of sample preparation was incomplete and that $NiCl_2$ was imbibed by zeolite Y during the exchange process.

Introduction

Microporous materials, especially the molecular sieves, are often used in heterogeneous catalysis. The faujasite-type zeolites X and Y are among the most used and studied. One way to modify these zeolites, to optimize their properties for particular applications, is to replace some or all of their exchangeable cations with those of another element. The thermal stability, sorption characteristics, and catalytic properties of a zeolite depend on the type and number of exchangeable cations it contains and their distribution over the available sites. Important to both catalysis and sorption is the accessibility of these cations to guest molecules.

Ion exchange is commonly done from aqueous solution, but alternative methods of introducing cations, such as solid-state ion exchange (SSIE), may be more convenient. SSIE in zeolites was first described by Rabo et al.[1,2] and Clearfield et al.[3] In recent years, the replacement of cations in zeolites via SSIE has attracted increased attention,[4−7] but to date no crystallographic investigations of the structures of these materials have been reported.[5]

The SSIE procedure is simple. Finely dispersed powders of a zeolite (e.g., NH_4−Y) and a compound (e.g., $ZnCl_2$) of the ingoing cation (Zn^{2+} in this example) are intimately mixed and heated to a relatively high temperature (550−1000 K).[3] Ideally the process results in the formation of the desired metal zeolite and the evolution of gases (NH_3, HCl, and H_2O, following the above example). Low-alumina zeolites such as zeolite Y are acid stable and are therefore suitable for SSIE.

SSIE has the following advantages[4] over conventional ion exchange from aqueous media: (i) it does not require the handling of large volumes of salt solution, (ii) it minimizes or avoids the problem of discarding waste salt solution, and (iii) it allows metal cations (which are small) to be introduced through narrow windows or channels that would impede or prevent ion exchange of solvated cations (which are larger) from aqueous solution.

Among the factors that affect the degree of exchange by SSIE are the structure type of the zeolite, the treatment temperature, the initial amount of salt in relation to the capacity of the zeolite, and the nature of the products formed. It has been shown that the reaction of various Ni and Mn salts with H−ZSM-5 zeolite depends on the nature of the anion.[4] The highest degrees of exchange were reached with metal chlorides, where hydrochloric acid is released into the gas phase without affecting the integrity of the zeolite structure. Higher temperatures have been shown to increase the degree of exchange. It has been reported that the degree of exchange for the $CuCl_2/NH_4$−Y system is considerably higher than for $CuCl_2$/H−ZSM-5 at 670 K.[4] A greater excess of the metal chloride results in a higher degree of exchange. Volatile (gaseous) products that can be removed easily from the system would drive the reaction toward the desired product: hence the extensive use of the chloride, which on reacting with hydrated NH_4−Y yields the gaseous products NH_3 and HCl.[5,7]

S1089-5647(97)03107-6 CCC: $15.00
Published on Web 03/20/1998

Previously, the structures of three Ni^{2+}−Y zeolites ion-exchanged from aqueous solution were studied using X-ray diffraction in order to determine the Ni^{2+} populations at the various cation sites as a function of both the extent of exchange and the degree of dehydration.[8] On the progressive removal of water, Ni^{2+} ions were found to occupy site I preferentially, with a limit of 12 ions per unit cell. Ni^{2+} ions were also found at two I′ sites. The level of exchange ranged from 14 to 19 Ni^{2+} ions per unit cell of initial composition $Na_{56}Si_{136}Al_{56}O_{384}$.

This work was an attempt to prepare fully Ni^{2+}-exchanged zeolite Y by SSIE methods. Both the structures of the fully dehydrated product and a partially rehydrated form were studied, to see the effect of hydration on the positions of the extraframework cations and to locate coordinated water molecules.

Experimental Section

Zeolite Y powder of composition $Na_{55}Si_{137}Al_{55}O_{384}$ was kindly provided by Royal Shell Laboratories, Amsterdam (KSLA). A 10 g sample was NH_4^+-exchanged by contact with a 5-fold excess of 1.0 M aqueous $NH_4C_2H_3O_2$ (Fisher Chem. Co., Certified ACS grade) with occasional stirring at 93 °C.[9] The solution was renewed five times, approximately daily. The slurry was then suction filtered, rinsed well with deionized water, and allowed to dry at 24 °C, followed by further drying at 50 °C to constant weight.

(a) Preparation of Ni_{30}−Y: A 4-fold excess of $NiCl_2 \cdot 6H_2O$ (Baker Chemical Co., 99.9%, 6.2 g) was added to 4.0 g of NH_4−Y powder in a mortar and ground well until a homogeneous mixture was produced. The mixture was then introduced into a Pyrex U-tube, placed in an oven and heated in air. The temperature was raised gradually over a period of 6 h to reach a final temperature of 425 °C. Heating was continued at this temperature for 18 h. Evolution of HCl was noted and monitored at regular intervals with pH paper. Heating was stopped when the color change on the pH paper was minimal. The contents were then allowed to return to room temperature and ground well once again in a mortar, and the above heating procedure was repeated. Finally, the contents were allowed to cool, washed quickly with deionized water (to remove excess nickel salt), and then suction filtered. The product was allowed to dry at room temperature, followed by further drying at 50 °C to constant weight.

A portion of the above product (3.9 g) was then dehydrated under vacuum. Initial dehydration at 24 °C was followed by gradually increasing the temperature to 400 °C over a period of 4 h. Heating was continued at this temperature until the pressure dropped to 1.2×10^{-4} Torr, followed by a further 24 h of heating at this temperature and pressure. After cooling to 24 °C, the tube containing the sample (Ni_{30}−Y) was sealed under vacuum.

(b) Preparation of Ni_{30}−Y·D_2O: To the above sample, Ni_{30}−Y, after neutron-diffraction data had been collected, 4.0 mL of D_2O (Aldrich Chemical Co., 99.9%) was added inside a helium (99.996%)-filled glovebag. After it had equilibrated for 0.5 h, it was quickly removed and attached to the vacuum system. Dehydration was carried out at 24 °C until the pressure had decreased to 1×10^{-6} Torr. After 12 h of evacuation at this pressure, the sample was sealed off from the vacuum system.

(c) Chemical analysis: Chemical analysis by ICP methods (Table 1) yielded a unit-cell content of 30 Ni ions and five to seven Na ions. This shows that, despite the exhaustive NH_4^+-exchange treatment that was done, Na^+ remained in Ni_{30}−Y (and therefore in Ni_{30}−Y·D_2O). A qualitative test with $AgNO_3$(aq) indicated a substantial chloride content. Taken together, the above indicate that substantial overexchange (imbibation of $NiCl_2$) had occurred during the solid-state ion-exchange process.

TABLE 1: Cation Composition of Ni_{30}−Y and Ni_{30}−Y·D_2O

	Al	Si	Ni	Na
		Analysis 1		
mg/g	81.6(33)	221.0(10)	96.1(6)	7.42(30)
molar ratio	3.02(13)	7.87(4)	1.63(1)	0.32(1)
	Si:Al = 2.61; number of Ni^{2+} ions = 29.9(2);[a] number of Na^+ ions = 5.80(24)[a]			
		Analysis 2		
mg/g	81.4(43)	222.0(2)	95.5(8)	7.44(110)
molar ratio	3.02(17)	7.90(2)	1.63(1)	0.32(16)
	Si:Al = 2.62; number of Ni^{2+} ions = 29.9(3);[a] number of Na^+ ions = 5.80(84)[a]			

[a] This value was calculated on the basis of Si:Al = 2.49, derived from the composition of the stock supply of Na−Y used initially. The mean of the values found above for Si:Al does not differ significantly from 2.49. If that mean, 2.615, was used, the mean number of Ni and Na ions would have been 28.3 and 5.6, respectively, not much different.

TABLE 2: Diffraction and Structure Refinement Data

	Ni_{30}−Y	Ni_{30}−Y·D_2O
chemical composition	$Ni_{30}Na_7Cl_{12}Al_{55}Si_{137}O_{384}$	Ni_{30}−Y·xD_2O
space group	*Fd*3*m*	*Fd*3*m*
a_0 at 15 K, Å	24.47565(27)	24.47198(30)
d-spacing range, Å	0.80−2.87	0.80−2.87
excluded regions, Å	1.06−1.07[a]	1.06−1.07[a]
	1.17−1.18	1.24−1.25[a]
	1.24−1.25[a]	1.75−1.76[a]
	1.44−1.45	2.02−2.03[a]
	1.75−1.77[a]	
	2.02−2.04[a]	
no. of observations	4171	4241
no. of reflections	1688	1687
no. of parameters	52	53
$R_p = \sum\|I_o - I_c\|/\sum I_o$	0.0212	0.0184
$R_{wp} = (\sum[w(I_o - I_c)^2]/\sum[wI_o^2])^{1/2}$	0.0287	0.0257

[a] These four regions bracket the four strongest powder diffraction lines of Ni metal.[20]

Gravimetric analysis for chloride yielded approximately 13 Cl ions per unit cell, in good agreement with the crystallographic results. The method[10] (modified) involved the decomposition of the zeolite sample in concentrated nitric acid, repeated washing of the product gels to extract all Cl^-, and adding $AgNO_3$ to the total solution to precipitate AgCl.

(d) Data collection and management: For the pulsed-neutron diffraction experiments, the samples were transferred in a helium (99.996%)-filled glovebag to vanadium cans fitted with indium seals. Diffraction data for each sample were gathered at 15 K for about 14 h on the GPPD (General Purpose Powder Diffractometer) instrument of the IPNS (Intense Pulsed Neutron Source) at ANL (Argonne National Laboratory).

Data from the $2\theta = 148°$ banks of detectors were processed and analyzed by GSAS (General Structure Analysis System),[11] a menu-driven graphical software system that uses Rietveld refinement techniques.[12] Unfortunately, an absorption correction was not done, so the thermal parameters reported are likely to be inaccurate. Table 2 provides a summary of the crystallographic data and data-collection parameters.

Several regions were excluded from Rietveld refinement in both powder diffraction intensity profiles (see Table 2). The relatively wide nonzeolitic peaks seen in these regions can be attributed nearly entirely to finely divided Ni metal. Ni may

TABLE 3: Positional, Thermal, and Occupancy Parameters

atom	Wyckoff position	*x*	*y*	*z*	U_{11}[b] or U_{iso}	U_{22}	U_{33}	U_{12}	U_{13}	U_{23}	occupancy[c] varied	occupancy[c] fixed
					(a) $Ni_{30}-Y$[a]							
Si,Al	192(i)	-5327(17)	3594(23)	12476(18)	0.5(8)							192
O(1)	96(h)	−10283(17)	10283(17)	0	22(2)	22(2)	12(3)	0(3)	−25(2)	−25(2)		96
O(2)	96(g)	−12(22)	−12(22)	14420(23)	46(3)	46(3)	40(4)	33(4)	5(3)	5(3)		96
O(3)	96(g)	17932(17)	17932(17)	−2699(28)	47(3)	47(3)	50(5)	−6(3)	−23(2)	−23(2)		96
O(4)	96(g)	17425(21)	17425(21)	32122(28)	25(2)	25(2)	54(5)	26(2)	−41(3)	−41(3)		96
Ni(I)	16(c)	0	0	0	28.5[d]						2.9(3)	4
Ni(I′)	32(e)	5568(33)	5568(33)	5568(33)	28.5[d]						12.0(2)	12
Ni(I″)	32(e)	7503(67)	7503(67)	7503(67)	28.5[d]						6.0(2)	6
Ni(II′)	32(e)	20864(42)	20864(42)	20864(42)	28.5[d]						9.0(4)	8
Cl	96(g)	15231(55)	15231(55)	18180(108)	28.5[d]						11.9(5)	12
					(b) $Ni_{30}-Y\cdot D_2O$[a]							
Si,Al	192(i)	−5284(19)	3555(24)	12682(22)	7(1)							192
O(1)	96(h)	−10468(19)	10468(19)	0	39(3)	39(3)	67(6)	20(4)	−41(3)	−41(3)		96
O(2)	96(g)	−126(23)	−126(23)	14470(20)	−44(3)	−44(3)	8(3)	30(3)	12(2)	12(2)		96
O(3)	96(g)	17640(17)	17640(17)	−3173(30)	24(2)	24(2)	90(6)	−3(3)	−25(3)	−25(3)		96
O(4)	96(g)	17497(19)	17497(19)	32467(35)	23(2)	23(2)	63(5)	5(3)	−30(2)	−30(2)		96
Ni(I)	16(c)	0	0	0	25.0[d]						4.2(3)	4
Ni(I′)	32(e)	7439(36)	7439(36)	7439(36)	25.0[d]						11.2(3)	11
Ni(II′)	32(e)	19834(123)	19834(123)	19834(123)	25.0[d]						3.6(4)	4
Ni(III′)	96(g)	30700(82)	30700(82)	9495(104)	25.0[d]						11.2(5)	11
W	96(g)	7275(53)	7275(53)	15521(51)	25.0[d]						29.2(8)	27
D	96(g)	−2634(108)	−2634(108)	20681(144)	11.0[d]						11.2(5)	11

[a] Origin at $\bar{3}m$. Positional parameters ($\times 10^5$) and anisotropic thermal parameters (Å^2 $\times$ 10^3) are given. Numbers in parentheses are esd's in the units of the least significant digit given for the corresponding parameter. [b] The anisotropic temperature factor = $\exp\{(-2\pi^2/a^2)(h^2U_{11} + k^2U_{22} + l^2U_{33} + 2hkU_{12} + 2hlU_{13} + 2klU_{23})\}$. [c] Occupancies are given as the number of atoms or ions per unit cell. [d] Fixed values.

have formed by the reduction of $NiCl_2$ by the NH_3 evolved during the SSIE process. It may generally be expected that metals with positive or small negative standard reduction potentials will be reduced by NH_3 during SSIE of NH_4^+ zeolites. These reduced metals may be catalytically active.

The coherent neutron scattering lengths used were Si, 4.15; Al, 3.45; O, 5.81; Ni, 10.3; Cl, 9.4; and D, 6.67 fm.

Structure Determination

(a) $Ni_{30}-Y$: Full-matrix least-squares refinement was initiated in the space group *Fd*3*m* using the atomic parameters of the zeolite framework ((Si,Al), O(1), O(2), O(3), and O(4)) of dehydrated Zn−Y.[9] Since the SiO_4 and AlO_4 tetrahedra are indistinguishable in this space group, only the average species (Si,Al) is considered in this work. Initial anisotropic refinement of the framework oxygens and isotropic refinement at (Si,Al) converged with $R_p = 0.0278$ and $R_{wp} = 0.0386$.

An ensuing difference Fourier function revealed several peaks, the two largest of which were refined by least-squares analysis. This refinement led to the location of Ni(I) at site I and Ni(I′) at site I′ (see Table 3a). At convergence, R_p and R_{wp} had decreased to 0.0230 and 0.0313, respectively. A second difference Fourier function revealed more peaks: the largest, at site II′, was included in the least-squares for refinement as Ni(II′). This led to convergence with $R_p = 0.0219$ and $R_{wp} = 0.0300$.

A peak from a third difference Fourier function was refined as Cl. At convergence, the error indexes were further lowered to $R_p = 0.0216$ and $R_{wp} = 0.0293$ with an occupancy of 11.9(5) at Cl, insignificantly different from the number of chloride ions per unit cell (13) obtained by gravimetric analysis. A fourth Ni position at a second site I′ (designated as I″) was found on a subsequent difference Fourier function. Inclusion of this peak as Ni(I″) led to convergence and to a further reduction in *R*'s: $R_p = 0.0211$ and $R_{wp} = 0.0286$. The total Ni occupancy at this stage of refinement was in the range 29.5−31.3, and the Cl occupancy was 11.9(5).

During the above refinements, the Ni(I″), Cl, and Ni(I′) occupancies showed a close 1:2:2 relationship. Hereafter least-squares included that as a constraint. Allowing the thermal parameters of the extraframework atoms to vary (with and without constraints) led to unreasonable occupancies that did not sum to the Ni content based on analysis. To correct this problem, the thermal parameters of all extraframework atoms were kept fixed at $U = 0.0285$ Å^2, a reasonable value. (High correlation was seen in least-squares between thermal parameters and occupancies.) Least-squares refinement with nonframework occupancies varying led to convergence and to the error indexes $R_p = 0.0211$ and $R_{wp} = 0.0286$.

The Ni^{2+} occupancy of nine at site II′ (see Table 3a) was unacceptable because it would require one too-short Ni(II′)−Ni(I′) contact of 3.79 Å; it was fixed at eight, its maximum reasonable value. Also, because four Ni^{2+} ions were found at site I in $Ni_{30}-Y\cdot D_2O$ (vide infra), and to preserve the count of Ni^{2+} ions per unit cell at 30, the occupancy at Ni(I) was increased from ca. three to four.

The site occupancies of all nonframework ions were held fixed in the final cycles of refinement (see Table 3a); at convergence, the error indexes were $R_p = 0.0212$ and $R_{wp} = 0.0287$. The final atomic coordinates are presented in Table 3a and selected bond distances and angles are in Table 4. Figure 1 shows the agreement between the calculated and the observed peak profile intensities.

Conventional background scattering was fitted with a 12-parameter analytical function, and three parameters were allowed to vary to fit a 12-parameter peak-shape function.[13] Additional experimental and refinement details may be found in Table 2.

(b) $Ni_{30}-Y\cdot D_2O$: Full-matrix least-squares refinement was initiated as above.[9] Initial anisotropic refinement of the framework oxygens and isotropic refinement of (Si,Al) converged with $R_p = 0.0256$ and $R_{wp} = 0.0363$.

An ensuing difference Fourier function revealed several peaks, the two largest of which were refined by least-squares. This refinement led to the location of Ni(I) at site I and Ni(I′) at site

TABLE 4: Selected Interatomic Distances (Å) and Angles (deg)[a]

	Ni_{30}−Y	Ni_{30}−Y·D_2O
(Si,Al)-O(1)	1.592(5)	1.631(6)
(Si,Al)-O(2)	1.643(5)	1.611(6)
(Si,Al)-O(3)	1.700(6)	1.682(6)
(Si,Al)-O(4)	1.616(5)	1.615(6)
O(1)−(Si,Al)-O(2)	113.8(4)	113.7(4)
O(1)−(Si,Al)-O(3)	107.6(4)	106.1(4)
O(1)−(Si,Al)-O(4)	112.3(4)	106.9(5)
O(2)−(Si,Al)-O(3)	101.2(4)	106.2(4)
O(2)−(Si,Al)-O(4)	108.8(4)	113.0(5)
O(3)−(Si,Al)-O(4)	112.7(4)	111.1(5)
(Si,Al)-O(1)−(Si,Al)	145.0(5)	143.3(5)
(Si,Al)-O(2)−(Si,Al)	140.1(5)	143.3(6)
(Si,Al)-O(3)−(Si,Al)	129.5(5)	139.7(7)
(Si,Al)-O(4)−(Si,Al)	146.2(6)	139.7(7)
Ni(I)-O(3)	2.534(6)	2.663(6)
Ni(I′)-O(3)	2.089(7)	2.597(12)
Ni(I′)-Cl	2.597(13)	
Ni(I′)-W		1.979(16)
Ni(I′)-W1		2.247(10)
Ni(I″)-O(3)	2.502(19)	
Ni(I″)-Cl	2.73(4)	
Ni(II′)-O(2)	2.133(7)	2.253(18)
Ni(III′)-O(1)		1.834(5)
Ni(III′)-O(2)		2.281(26)
Ni(III′)-O(3)		1.650(23)
Ni(III′)-D		2.94(4)
D−O(2)		1.75(4)
Cl−O(2)	2.927(22)	
Cl−O(3)	3.140(21)	
Cl−Cl	2.91(4)	
O(3)−Ni(I)-O(3)	83.7(2)	86.4(2)
	96.3(2)	93.6(2)
O(3)−Ni(I′)-O(3)	108.0(4)	89.0(4)
O(3)−Ni(I″)-O(3)	85.0(7)	
O(2)−Ni(II′)-O(2)	118.5(2)	109.8(12)
O(1)−Ni(III′)-O(1)		42.8(4)
O(1)−Ni(III′)-O(2)		121.8(17)
O(1)−Ni(III′)-O(3)		81.7(8)
O(2)−Ni(III′)-O(3)		81.7(10)
O(3)−Ni(I′)-Cl	83.4(6)	
	101.7(10)	
	142.4(7)	
O(3)−Ni(I″)-Cl	104.6(3)	
	166.8(10)	
O(3)−Ni(I′)-W		89.3(4)
		177.7(8)
W−Ni(I′)-W		92.3(8)
W−Ni(I′)-W1		91.9(6)
Cl−Ni(I″)-Cl	64.5(10)	
Ni(I′)-Cl−Ni(I″)	102.6(15)	

[a] Numbers in parentheses are estimated standard deviations in the units of the least significant digit given for the corresponding value.

I′ (see Table 3b). At convergence, R_p and R_{wp} had decreased to 0.0215 and 0.0302, respectively.

A peak from a second difference Fourier function was refined as W (a D_2O oxygen atom) in least-squares (see Table 3b). At convergence, the error indexes had decreased to $R_p = 0.0193$ and $R_{wp} = 0.0267$. The addition of two more peaks from a subsequent difference Fourier function as Ni(III′) and as D (both in the supercages) resulted in a further lowering of the error indexes to $R_p = 0.0185$ and $R_{wp} = 0.0258$. A final difference Fourier function revealed a peak at site II′ which was refined as Ni(II′). Least-squares refinement with nonframework occupancies varying converged to $R_p = 0.0183$ and $R_{wp} = 0.0256$.

Allowing the thermal parameters of the extraframework atoms to vary isotropically, independently, or with the constraint that the thermal parameters of the Ni atoms be equal, led to a total Ni population of about 36, more than the value of 30 required by chemical analysis. Therefore, the thermal parameters were adjusted and fixed at reasonable values (Table 3b) as in Ni_{30}−Y. During the initial refinement of the positional and fractional occupancy parameters of the extraframework atoms, the fractional occupancies of Ni(I′) and W (O of D_2O) showed a 1:3 relationship and those of Ni(III′) and D, a 1:1 relationship. Constraints were placed on these occupancies to maintain these relationships during subsequent refinement cycles.

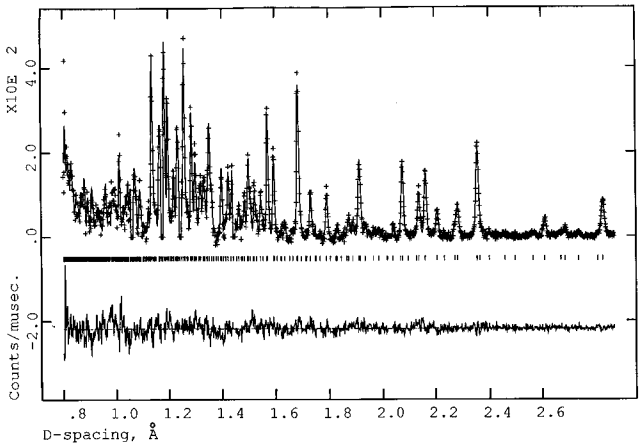

Figure 1. Observed, calculated, and difference pulsed-neutron powder diffraction profiles for Ni_{30}−Y. For clarity, the calculated background has been subtracted from both the observed and calculated profiles.

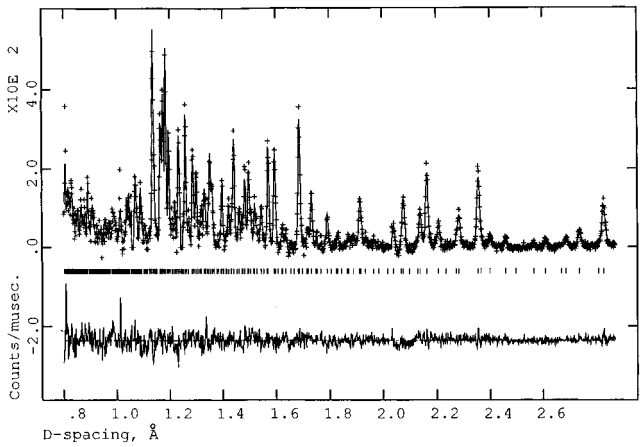

Figure 2. Observed, calculated, and difference pulsed-neutron powder diffraction profiles for Ni_{30}−Y·D_2O. For clarity, the calculated background has been subtracted from both the observed and calculated profiles.

The 11 Ni^{2+} ions at site I′ must fit into the eight sodalite units per unit cell. A relatively even distribution of these would require that three sodalite units have two Ni(I′) ions. Because this leads to two W−W contacts of ca. 0.8 Å, each such pair was replaced with a single W1 water oxygen at the average position, at 0.0728, 0.0845, and 0.1655, to give two bridging oxygens between the two Ni(I′) ions in those sodalite units. The number of molecules at W was then fixed at 27. The site occupancies of the remaining nonframework atoms and ions were also fixed (see Table 3b) in the final cycles of refinement. The final residuals were $R_p = 0.0184$ and $R_{wp} = 0.0257$. The final atomic coordinates are presented in Table 3b and selected bond distances and angles are in Table 4. Figure 2 shows the agreement between the calculated and the observed peak profile intensities.

Conventional background scattering was fitted with a 12-parameter analytical function, while all 12 parameters of the peak-shape function[13] were kept fixed at values found previously

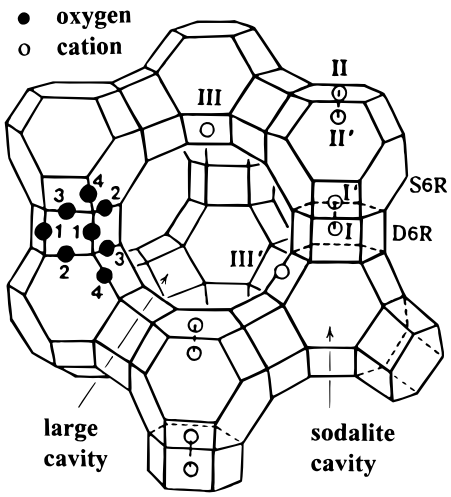

Figure 3. Stylized drawing of the framework structure of zeolite Y. Near the center of each line segment is an oxygen atom. The different oxygen atoms are indicated by the numbers 1−4. Silicon (or aluminum) atoms are at the tetrahedral intersections. Extraframework cation positions are labeled with Roman numerals.

at the IPNS for samples of zeolite Y. Additional experimental and refinement details may be found in Table 2.

Discussion

Zeolite Y is a synthetic counterpart of the naturally occurring mineral faujasite. The 14-hedron with 24 vertexes known as the sodalite cavity or β cage may be viewed as the building block of the aluminosilicate framework of the zeolite (see Figure 3). These β-cages are connected tetrahedrally at 6-rings by bridging oxygens to give double 6-rings (D6R's, hexagonal prisms), and, concomitantly, to give an interconnected set of even larger cavities (α-cages, supercages) accessible in three dimensions through 12-ring (24-membered) windows. The Si and Al atoms occupy the vertexes of these polyhedra. The oxygen atoms lie approximately halfway between each pair of Si and Al atoms but are displaced from those points to give near-tetrahedral angles about Si and Al.

Exchangeable cations, which balance the negative charge of the aluminosilicate framework, are found within the zeolite's cavities. They are usually found at the following sites shown in Figure 3: site I, at the center of a D6R, is surrounded by an octahedron of oxygens; site I′, in the sodalite cavity on the opposite side of one of the D6R's 6-rings from site I, is close to three framework oxygens; site II′, in the sodalite cage near a single 6-ring (S6R) entrance to the supercage, is close to three framework oxygens; site II is in the supercage adjacent to a S6R; site III is on a 2-fold axis in the supercage opposite a 4-ring between 12-rings; finally site III′ is at an ill-defined general position near supercage or 12-ring oxygens, perhaps near site III, perhaps in or opposite a 4-ring adjacent to that at site III.

The initial composition of the Na−Y sample used, $Na_{55}Si_{137}Al_{55}O_{384}$ per unit cell exclusive of water molecules (analysis by Royal Shell Laboratories, Amsterdam (KSLA)), indicates that 55 positive charges are needed per unit cell to balance the anionic framework. This and the results of refinement at Cl (Table 3a), which agrees closely with the gravimetric analysis for chloride, and the duplicate chemical analyses for cations (Table 1) indicate the following composition for the fully dehydrated Ni^{2+}-exchanged sample: $Ni_{30}Na_7Cl_{12}Si_{137}Al_{55}O_{384}$. The net exchange reactions per unit cell can therefore be written as

aqueous:

$$Na_{55}-Y + 48\ NH_4^+ \rightarrow Na_7(NH_4^+)_{48}-Y + 48\ Na^+$$

followed by

SSIE:

$$Na_7(NH_4^+)_{48}-Y + 30\ NiCl_2 \rightarrow Ni_{30}Na_7Cl_{12}-Y + 48\ NH_3 + 48\ HCl$$

exclusive of water molecules. Despite the repeated high-temperature exchanges employed in the preparation of NH_4^+-exchanged zeolite Y, it is clear that only 48 of the 55 Na^+ ions per unit cell had been replaced. In addition, six molecules of $NiCl_2$ were imbibed per unit cell by the zeolite during the SSIE process.

(a) Zeolite Y framework: In both structures, the Si,Al−O(3) distances are the longest. Ni^{2+} ions preferentially coordinate to O(3) (18 in $Ni_{30}-Y$ and 22 in $Ni_{30}-Y{\cdot}D_2O$) and are responsible for this effect. Olson et al. noted this in 1968 in calcined Ce^{3+}-exchanged faujasite;[14] it is commonly seen in other structures such as $Mg_{46}-X$,[15] $Ca_{46}-X$,[15] $Ba_{46}-X$,[16] $Cd_{46}-X$[16], and $Mn_{46}-X$.[17]

(b) $Ni_{30}-Y$: Twelve Ni^{2+} ions per unit cell are found at site I′. Each coordinates to three O(3) framework oxygens at 2.089(7) Å and to one Cl^- ion at 2.597(13) Å in a distorted tetrahedral manner (see Figure 4). For comparison, the sums of the corresponding radii[18] are 0.69 + 1.32 = 2.01 Å and 0.69 + 1.81 = 2.50 Å, respectively. Ni(I′) extends 0.59 Å into the

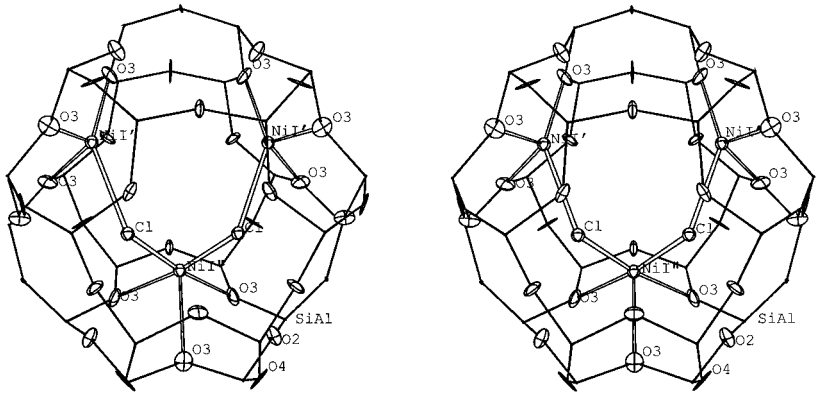

Figure 4. Stereoview of the sodalite unit in $Ni_{30}-Y$ showing the $[Ni_3Cl_2]^{4+}$ cluster. The zeolite framework is drawn with solid bonds between tetrahedrally coordinated (Si,Al) and oxygen atoms. Broad open bonds are shown between the Cl^- ions and the Ni^{2+} ions at sites I′ and I″ (bonds within the cluster). Narrow open bonds show the coordination of the Ni^{2+} ion at site I″ to the framework oxygens. Ellipsoids of 20% probability are shown.

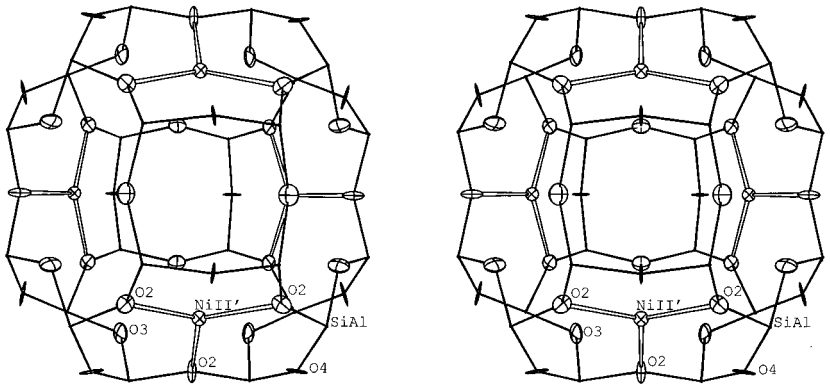

Figure 5. Stereoview of the sodalite unit in $Ni_{30}-Y$ showing the coordination of Ni^{2+} at site II′ to three framework oxygens. The zeolite framework is drawn with solid bonds between tetrahedrally coordinated (Si,Al) and oxygen atoms. Open bonds are shown between Ni^{2+} and the framework oxygens. Ellipsoids of 20% probability are shown.

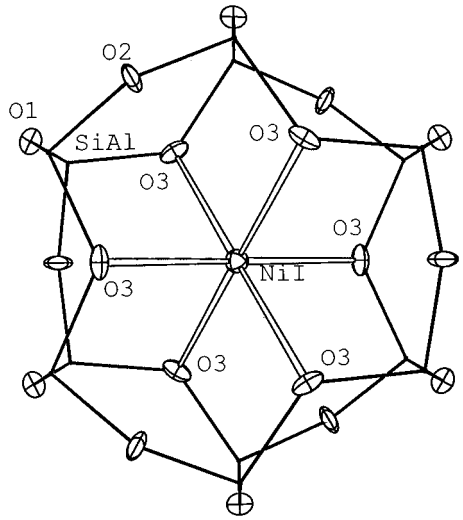

Figure 6. Double 6-ring (D6R) in $Ni_{30}-Y$ showing a Ni^{2+} ion at site I. The zeolite framework is drawn with solid bonds between tetrahedrally coordinated (Si,Al) and oxygen atoms. Open bonds show the coordination of Ni^{2+} to the six nearest oxygens. Ellipsoids of 20% probability are shown.

sodalite unit from the plane of the three O(3) oxygens to which it coordinates.

Six Ni^{2+} ions per unit cell are found at another I′ site, here called site I″. Each coordinates to three O(3) framework oxygens at 2.502(19) Å (a surprisingly long distance) and to two Cl^- ions at 2.73(4) Å in an irregular five-coordinate manner (see Figure 4 and Table 4). O(3)−Ni(I″)−O(3) is 85.0(7)° and Cl−Ni(I″)−Cl = 64.5(10)°. Ni(I″) is 1.41 Å from its O(3) plane.

Eight Ni^{2+} ions per unit cell are found at site II′. Each coordinates only to three O(2) framework oxygens: Ni(II′)−O(2) = 2.133(7) Å and O(2)−Ni(II′)−O(2) = 118.5(2)° (see Figure 5). Each is only 0.26 Å from the O(2) plane of its S6R.

Four Ni^{2+} ions have been placed at site I. Each coordinates octahedrally to six framework oxygens (see Figure 6) at 2.534-(6) Å, a distance substantially greater than the sum of the ionic radii,[18] 2.01 Å. The two unequal angles at Ni(I), O(3)−Ni-(I)−O(3) = 83.7(2)° and 96.3(2)°, indicate that the coordination octahedron is 3-fold-axially distorted; it is prolate.

The relative occupancies at Ni(I′), Ni(I″) and Cl (see Table 3a) are consistent with the formation of a $(NiClNiClNi)^{4+}$ cluster (see Figure 4) in six of the eight sodalite cages per unit cell. Because the Ni(I″)−O(3) distance, 2.502(19) Å, is substantially longer than Ni(I′)−O(3), 2.089 (7) Å, the central three atoms of the $(NiClNiClNi)^{4+}$ cluster may have some of the characteristics of a neutral molecule. This is not seen in the Ni−Cl bond lengths, however, which do not differ significantly.

The four Ni^{2+} ions at site I occupy 4 of the 16 available D6R's per unit cell. To avoid two too-short $Ni^{2+}-Ni^{2+}$ repulsions (Ni(I)-Ni(I′) = 2.36 Å and Ni(I)−Ni(I″) = 3.18 Å), no I′ or I″ Ni^{2+} ions should approach these four D6R's. The 12 Ni(I′) and 6 Ni(I″) ions must then share the remaining 12 D6R's, and some doubling up is necessary. A Ni(I′)−Ni(I′) repulsion of 4.72 Å may also be avoided. It follows that 6 of the 12 D6R's have a Ni(I′) ion on one side and a Ni(I″) on the other (Ni(I′)−Ni(I″) = 5.54 Å). It is to minimize this repulsion that Ni(I″), which bonds to two Cl^- ions, is pushed so deeply into the sodalite cavity by Ni(I′), which bonds to only one Cl^- ion and so requires closer coordination to O(3) oxygens. The remaining six D6R's host only one Ni(I′) ion.

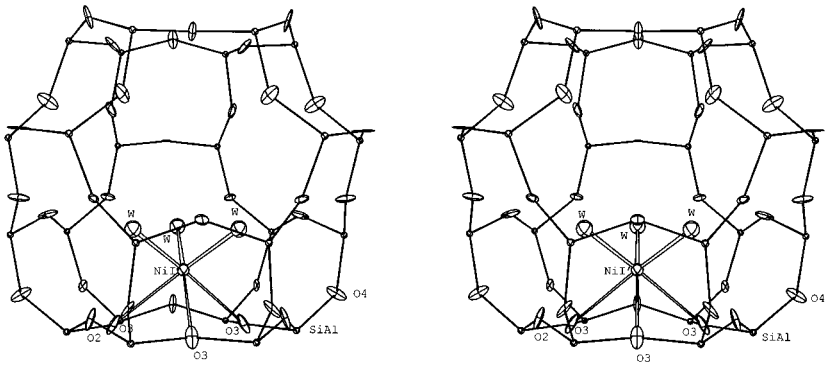

Figure 7. Stereoview of a sodalite unit in $Ni_{30}-Y\cdot D_2O$ showing the octahedrally coordinated Ni^{2+} ion at site I′. The zeolite framework is drawn with solid bonds between the tetrahedrally coordinated (Si,Al) and oxygen atoms. Open bonds show the coordination of Ni^{2+} to the D_2O and framework oxygens. Ellipsoids of 20% probability are shown.

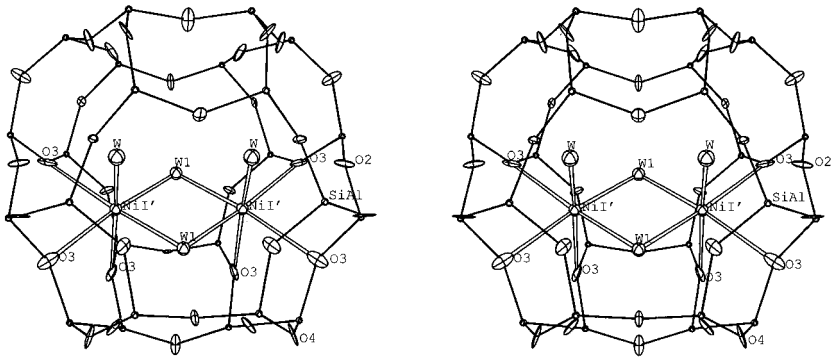

Figure 8. Stereoview of those ca. three sodalite units per unit cell in $Ni_{30}-Y\cdot D_2O$ which contain two Ni^{2+} ions at I′ sites. See the Figure 7 caption for further details.

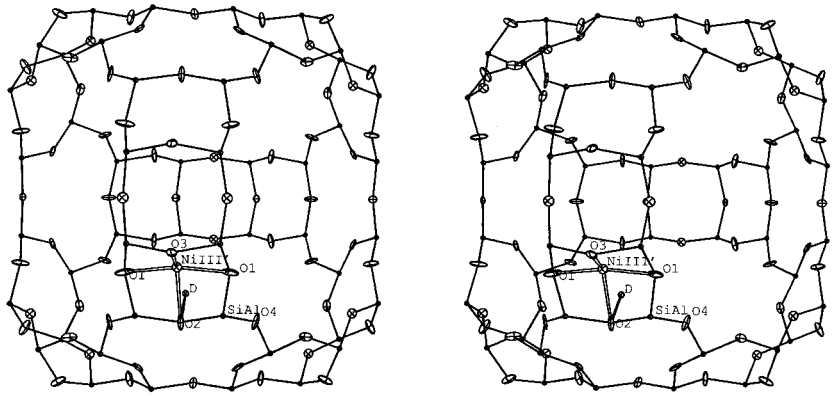

Figure 9. Stereoview of the large cavity of $Ni_{30}-Y\cdot D_2O$ showing the Ni^{2+} ion at site III′ coordinated to four framework oxygens and a deuterium atom (of an otherwise unlocated D_2O) bonded to a framework oxygen. The zeolite framework is drawn with solid bonds between the tetrahedrally coordinated (Si, Al) and oxygen atoms. Open bonds are shown between Ni^{2+} and the framework oxygens and between D and a framework oxygen. Ellipsoids of 20% probability are shown.

The eight Ni(II′) ions must then fully occupy all of the II′ sites in the two remaining sodalite units per unit cell, whose I′ sites are all empty (see Figure 5). In this way the Ni(I′)−Ni(II′) repulsions of 3.78 Å and the Ni(I′′)−Ni(II′) repulsions of 3.47 Å are avoided. The closeness of Ni(II′) to the plane of the three O(2) oxygens is consistent with this arrangement: the inter-Ni(II′) distances are 5.79 Å.

The ca. seven Na^+ ions per unit cell were not found. Perhaps this is because the scattering length for Na is smaller than that for any other atom in this structure. They could be accommodated at sites III or III′ in the supercage.

(c) $Ni_{30}-Y\cdot D_2O$: Eleven Ni^{2+} ions per unit cell are found at site I′. Distributing these relatively evenly among the eight sodalite units would put one in each of five sodalite units and two in each of the remaining three. Each of the five single Ni(I′) ions coordinates to three O(3) framework oxygens at 2.597(12) Å and to three D_2O (W) molecules at 1.979(16) Å in a distorted octahedral manner (see Figure 7 and Table 4). The remaining six Ni(I′) ions (three pairs) each coordinates octahedrally to one terminal D_2O molecule, two bridging D_2O molecules (W1), and three framework oxygens; Ni(I′)−W1 = ca. 2.25 Å (see Figure 8). W−Ni(I′)−W1 is 91.9(6)°, insignificantly less than W−Ni(I′)−W (92.3(8)°) formed by the octahedral Ni(I′) ions in the other five sodalite units (see Figures 7 and 8). Ni(I′) extends 1.52 Å into the sodalite unit from the plane of the three O(3) oxygens to which it is coordinated.

Eleven Ni^{2+} ions are found at site III′, a supercage site nearly in the plane of a 4-ring. Each coordinates to four framework oxygens in a distorted square-planar manner; Ni(III′) is 1.834(5) Å from two O(1) oxygens, 2.281(26) Å from an O(2) oxygen, and 1.650(23) Å (unrealistically small) from an O(3) oxygen (see Figure 9). The Ni(III′) ions must distort their

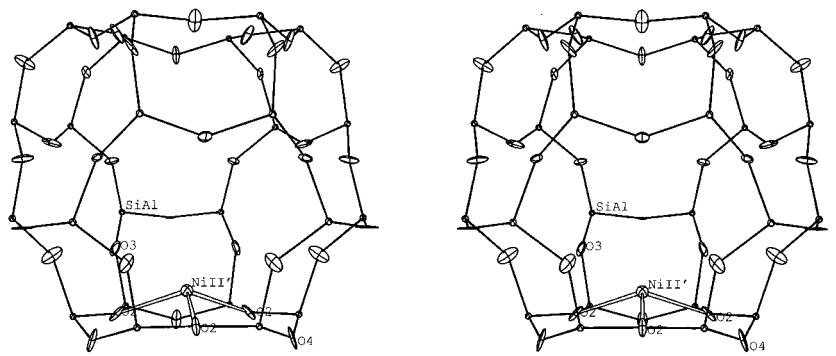

Figure 10. Stereoview of a sodalite unit in $Ni_{30}-Y\cdot D_2O$ showing the coordination of Ni^{2+} at site II′ to three framework oxygens. See the Figure 5 caption for further details.

immediate environments, which here are likely to be representative of the majority (empty) 4-rings, to give a more reasonable geometry. Eleven deuterium (D) atoms are close to one of these framework oxygens (D−O(2) = 1.75(4) Å, a typical O- - -H hydrogen-bonding distance) and 2.94(4) Å from Ni(III′). This indicates that each Ni(III′) ion coordinates axially to a D_2O molecule (whose oxygen and remaining deuterium atom remain unlocated) (see Figure 9).

Four Ni^{2+} ions are found at site II′, 2.253(18) Å from three O(2) framework oxygens. O(2)−Ni(II′)−O(2) is 109.8(12)° (see Figure 10). Each Ni(II′) ion may be expected to coordinate to one or more D_2O molecules (not found) to satisfy its coordination requirements. Ni(II′) is 0.74 Å from the O(2)-plane of its S6R.

Four Ni^{2+} ions are found at site I. Each coordinates octahedrally to six framework oxygens as in Figure 6 at 2.663(6) Å. The two unequal angles at Ni(I), O(3)−Ni(I)−O(3) = 86.4(2)° and 93.6(2)°, indicate that this octahedron is 3-fold-axially distorted. As in Ni_{30}−Y, it is prolate.

The four Ni(I) ions occupy four of the available D6R's per unit cell. To avoid a short Ni^{2+}−Ni^{2+} repulsion (Ni(I)−Ni(I′) = 3.15 Å), Ni(I′) ions should not approach these four D6R's. After the 11 Ni(I′) ions are placed as described above, adequate space remains for the four Ni(II′) ions in those sodalite units that contain only one Ni(I′) ion; Ni(I′)−Ni(II′) = 5.25 Å.

To summarize, three of the sodalite units would have two Ni(I′) ions each, four would have one Ni(I′) and one Ni(II′) ion, and one would have just one Ni(I′) ion.

Many atoms remain unlocated in this structure. As in Ni_{30}−Y, the Na^+ ions were not found. In addition, the Cl^- ions and many of the D_2O molecules could not be found.

(d) Comparisons of structures: The Ni occupancy of four at site I in the anhydrous structure is apparently preserved even after rehydration. The long bond distances between framework oxygens and the Ni^{2+} ions at site I″ in Ni_{30}−Y and those at site I′ in Ni_{30}−Y·D_2O can be attributed to increased coordination by the guest species Cl^- and D_2O. The number of Ni^{2+} ions at sites I′ and II′ have been substantially reduced (from 12 + 6 = 18 to 11, and from 8 to 4, respectively) by D_2O sorption; these 11 Ni^{2+} ions ((18−11) + (8−4)) have moved from the sodalite units in Ni_{30}−Y to a III′ site (a 4-ring site involving the 4-ring adjacent to that at site III) in the large cavities in Ni_{30}−Y·D_2O.

Work on zeolite Y Ni^{2+}-exchanged by aqueous methods had shown that Ni^{2+} shows a preference for site I which increases with increasing dehydration[8,16] to a maximum of 12 ions per unit cell. That work also showed that the unit-cell constants decrease with increasing dehydration. However, overexchanged Ni_{30}−Y and Ni_{30}−Y·D_2O, products of SSIE methods, do not show the above trend; whereas the site I population is relatively low and remains fixed, the unit-cell constant of Ni_{30}−Y (24.475 65 Å) is nearly the same as (slightly higher than) that of Ni_{30}−Y·D_2O (24.471 98 Å). Presumably this is because neither structure is empty: Ni_{30}−Y contains Cl^- ions and Ni_{30}−Y·D_2O contains both Cl^- and D_2O. Coordination by guest species may be the reason for the increase, compared to the results of aqueous ion-exchange,[8,19] in the Ni^{2+} population at all sites other than site I.

Acknowledgment. This work has benefited from the use of the Intense Pulsed Neutron Source at Argonne National Laboratory. This facility is funded by the U.S. Department of Energy, BES-Materials Science, under Contract W-31-109-Eng-38. Ray Thomas and James W. Richardson of the IPNS were of great assistance. Charles Fraley of the Hawaii Institute of Geophysics and Planetology (HIGP) performed the chemical analyses. Acknowledgment is made to the donors of the Petroleum Research Fund, administered by the American Chemical Society, Grant No. 29025-AC5, for the primary support of this research.

References and Notes

(1) Rabo, J. A.; Poutsma, M. L.; Skeels, G. W. in *Proc. 5th Int. Congr. Catal.*; Miami Beach, 1972, Hightower, J. W., Ed.; North-Holland: New York, 1973; p 1353.

(2) Rabo, J. A. In *Zeolite Chemistry and Catalysis*; Rabo, J. A., Ed.; ACS Monograph 171, American Chemical Society: Washington DC, 1976; p 332.

(3) Clearfield, A.; Saldarriaga, C. H.; Buckley, R. C. In *Proc. 3rd Int. Conf. Molecular Sieves*; Zürich, 1973, Recent Progress Reports, Uytterhoeven, J. B., Ed.; University of Leuven Press: 1973; p 241.

(4) Karge, H. G.; Wichterlova, B.; Beyer, H. K. *J. Chem. Soc., Faraday Trans. 1*, **1992**, *88*, 1345.

(5) Karge, H. G. In *Zeolite Microporous Solids: Synthesis, Structure and Reactivity*; Derouane, E. G., Lemos, F., Naccache, C., Ribeiro, F. R., Eds.; *352*, Series C: Mathematical and Physical Sciences; Kluwer Academic Publishers: Dordrecht, 1991; p 273.

(6) Lazar, K.; Borbley, G.; Beyer, H. K.; Karge, H. G. *J. Chem. Soc., Faraday Trans.* **1994**, *90*, 1329.

(7) Karge, H. G. In *Progress in Zeolite and Microporous Materials*; Chon, H., Ihm, S. K., Uh, Y. S., Eds.; *105*, *Part C*, Studies in Surface Science and Catalysis; Elsevier: Amsterdam, 1997.

(8) Gallezot, P.; Imelik, B. *J. Phys. Chem.* **1973**, *77*, 652.

(9) Peapples-Montgomery, P. B.; Seff, K. *J. Phys. Chem.* **1992**, *96*, 5962.

(10) Olson, A. R.; Koch, C. W.; Pimentel, G. C. *Introductory Quantitative Chemistry*; Freeman: San Francisco, 1956; p 139.

(11) Larson, A. C.; Von Dreele, R. B. *General Structure Analysis System*; Los Alamos National Laboratory, LAUR 86-748, 1986.

(12) Rietveld, H. M. *J. Appl. Crystallogr.* **1969**, *2*, 65.

(13) Von Dreele, R. B.; Jorgensen, J. D.; Windsor, C. G. *J. Appl. Crystallogr.* **1982**, *15*, 581.

(14) Olson, D. H.; Kokotailo, G. J.; Charnell, J. *J. Colloid Interface Sci.* **1968**, *28*, 305.

(15) Yeom, Y. H.; Jang, S. B.; Kim, Y.; Song, S. W.; Seff, K. *J. Phys. Chem. B* **1997**, *101*, 6914.

(16) Yeom, Y. H.; Song, S. H.; Kim, Y.; Seff, K. *J. Phys. Chem. B* **1997**, *101*, 2138.

(17) Jang, S. B.; Jeong, M. S.; Kim, Y.; Seff, K. *J. Phys. Chem. B* **1997**, *101*, 9041.

(18) *Handbook of Chemistry and Physics*, 72nd ed.; Lide, D. R., Ed.; CRC Press: Boca Raton, FL, 1991/1992; p 12−8.

(19) Olson, D. H. *J. Phys. Chem.* **1968**, *72*, 4366.

(20) Powder Diffraction File, Search Manual (Inorganic Compounds), Fink Method, 1978; Joint Committee for Powder Diffraction Standards (JCPDS), International Center for Diffraction Data, Pennsylvania.